

***ten^m*, a *Drosophila* gene related to tenascin, is a new pair-rule gene**

**Stefan Baumgartner¹, Doris Martin,
Carmen Hagios and
Ruth Chiquet-Ehrismann**

Friedrich Miescher-Institut, Postfach 2543, CH-4002 Basel,
Switzerland

¹Corresponding author

Communicated by M.Noll

We describe the molecular characterization of the *Drosophila* gene *ten^m*, a large transcription unit spanning >110 kb of DNA. *ten^m* encodes a large extracellular protein of 2515 amino acids related to the extracellular matrix molecule tenascin. The Ten^m protein is found in seven stripes during the blastoderm stage, and each stripe overlaps with the *even-skipped* stripes. *ten^m* mutants show a phenotype resembling that of *odd-paired* (*opa*), a member of the pair-rule class of segmentation genes. Thus, Ten^m is the first example of a pair-rule gene product acting from outside the cell. While the Ten^m protein is under the control of *fushi tarazu* and *even-skipped*, but not of *opa*, at least two pair-rule genes, *paired* (*prd*) and *sloppy paired* (*slp*), and all segment-polarity genes analysed to date are under the control of *ten^m*. Our data suggest that Ten^m initiates a signal transduction cascade which acts, via or in concert with *opa*, on downstream targets such as *prd*, *slp*, *gooseberry*, *engrailed* and *wingless*, leading to an *opa*-like phenotype.

Key words: *Drosophila*/pair-rule gene/signal transduction/tenascin/*ten^m*

Introduction

In the last decade, much attention has been drawn to the extracellular matrix (ECM) molecule tenascin. Tenascin (also termed tenascin-C) is a large glycoprotein of six identical subunits with a reported monomer M_r of 190–320 kDa, depending on the species and type of splice variant analysed. It was identified because of its distinctive tissue distribution during development; it is present at times and places of morphogenetic tissue interactions and movements (for review see Chiquet-Ehrismann, 1990). More than half of the tenascin molecule consists of fibronectin type III (FN III) repeats, of which several appear differentially spliced between the different isoforms of tenascin. The other sequence units found in tenascin are EGF-like repeats, which are joined N-terminally to the FN III repeats, and a domain that shows extensive homology to the globular part of β - and γ -fibrinogen which is located at the C-terminus. Three monomers are held together in a region harbouring four heptad repeats forming a triple-coiled coil structure, which is itself fixed

by interchain disulfide bridges. Two trimers are finally disulfide-linked forming the hexameric structure. The structural features of tenascin have been presented and discussed in several papers (Erickson and Bourdon, 1989; Erickson, 1993).

In order to delineate the function of tenascin, several cell culture-based assays for cell adhesion were performed (Spring *et al.*, 1989; Aukhil *et al.*, 1993), with the controversial finding that tenascin can either promote or inhibit this activity. For example, by using recombinant tenascin fragments and comparing their cell binding activities with those of intact tenascin, Spring *et al.* (1989) showed that the tenascin molecule can be dissected into opposing functional domains. Fusion proteins containing the region of the second last FN III repeat allowed cell attachment but no spreading. Conversely, the region including the EGF-like domains prevented cell adhesion.

Recent studies have identified a growing number of proteins that share the same domain structure with tenascin, such as restrictin (also termed tenascin-R; Nönerberg *et al.*, 1992) and the product of a tenascin-like gene located in the human MHC locus, termed tenascin-X (Matsumoto *et al.*, 1992, Bristow *et al.*, 1993). To date, very little is known about the function of these novel proteins. Restrictin can promote cell adhesion of neural cells, but does not promote neurite extension (Rathjen *et al.*, 1991). No functional data are available yet on the human tenascin-X gene, which is prominently expressed in fetal muscle and testis and at lower levels in fetal adrenal gland, kidney and lung (Gitelman *et al.*, 1992; Bristow *et al.*, 1993). However, it has been suggested that this gene has an essential function, since many cases of adrenal hyperplasia have been traced to gene deletions in close proximity to, but never within, the tenascin-like gene (Bristow *et al.*, 1993).

Recently, using homologous recombination, mutant mice with disrupted tenascin expression were generated (Saga *et al.*, 1992). Surprisingly, these mutated mice appear to develop normally, indicating that these tenascin-related molecules mentioned above may compensate for the absence of tenascin. However, subtle phenotypes may have arisen that were not detected in that analysis.

Searches for tenascin-like genes in *Drosophila* have revealed at least two loci that share common sequences with tenascin. A recent report has shown the presence of tenascin-type EGF-like repeats in the Ten^a protein (Baumgartner and Chiquet-Ehrismann, 1993); however, neither FN III repeats nor fibrinogen homology were found in this molecule. Although Ten^a does not show the characteristic structural features of tenascin, its expression pattern in the central nervous system, in muscle attachment sites and in the eye appears very similar to the expression of vertebrate tenascin.

In a search for further tenascin-like genes in *Drosophila*

we have now isolated and characterized the *ten^m* gene ('m' for major). It encodes a large ECM protein including eight tenascin-type EGF-like repeats and 11 FN III-like repeats, but no fibrinogen domain. Surprisingly, the Ten^m protein is found in seven stripes during the blastoderm and germband extension stages. Moreover, we show that *ten^m* mutants exhibit a pair-rule phenotype reminiscent of that of *odd-paired (opa)* (Jürgens *et al.*, 1984). In contrast to all other pair-rule genes isolated to date, the *ten^m* gene is not a transcription factor and acts on the outside of cells. Our data suggest that Ten^m initiates a signal transduction cascade which acts, via or in concert with *opa*, on downstream targets such as *paired (prd)*, *sloppy paired 1 (slp1)*, *gooseberry (gsb)*, *engrailed (en)* and *wingless (wg)*.

Results

Cloning, sequence analysis and properties of *ten^m*

In our attempt to find further tenascin-related genes in *Drosophila* apart from *ten^a* (Baumgartner and Chiquet-Ehrismann, 1993), we screened the *Drosophila* genome for sequences homologous to a probe coding for the EGF-like domain of Ten^a under low stringency conditions (McGinnis *et al.*, 1984). Several phage clones were recovered that hybridized to the region encoding the Ten^a EGF-like domain and were subsequently used to isolate a set of overlapping genomic and cDNA clones covering the whole *ten^m* transcription unit (Figure 1B, see also Materials and methods). The *ten^m* gene structure revealed a genomic region spanning >110 kb of DNA with at least five introns (Figure 1B).

Conceptual translation of the 7545 nt open reading frame yields a protein of 2515 amino acids with a deduced molecular size of 281 kDa (Figure 2A). At the N-terminus,

the predicted initiating methionine is followed by an amino acid sequence containing structural regions characteristic of a secretory signal sequence (Figure 2A; von Heijne, 1986). Since a hydropathy profile of the primary structure revealed no further long hydrophobic regions indicative of a membrane-spanning segment (Figure 2D), *ten^m* is likely to encode a putative secreted protein.

The most conspicuous characteristics of the protein are two domains each represented by a series of reiterated patterns of amino acids (Figure 2B and C). The first domain is a series of eight tenascin-type EGF-like repeats (represented by diamonds in Figure 2C). Each of these repeats is ~31 amino acids long. They show the characteristic spacing of six cysteine residues as observed in vertebrate tenascin (consensus repeat: X₄CX₃CX₅CX₄CX₁CX₈C; Pearson *et al.*, 1988) and in *Drosophila ten^a* (Baumgartner and Chiquet-Ehrismann, 1993). The Ten^m EGF-like repeats appear to be most highly related to the repeats of Ten^a, with respect to both the number of repeats and to irregularities within the repeats. The repeat sequence is 56% identical and 71% similar (if conservative changes are allowed) to the Ten^a EGF-like domains but only 42% identical to the chicken tenascin EGF-like domains. In addition, the two amino acids that replaced the two cysteine residues in the Ten^a EGF-like domain (Baumgartner and Chiquet-Ehrismann, 1993) are also replaced in Ten^m at identical relative positions (underlined amino acids in Figure 2B), indicating a close structural relationship between these two domains.

The majority of the Ten^m amino acid sequence (residues 734–2238) can be divided into 11 repeated structures similar to FN III repeats (represented by open squares in Figure 2C). The domains are characterized by conserved tryptophan and tyrosine residues that are separated by 41–48 amino acids (Figure 2B). Other amino acids within

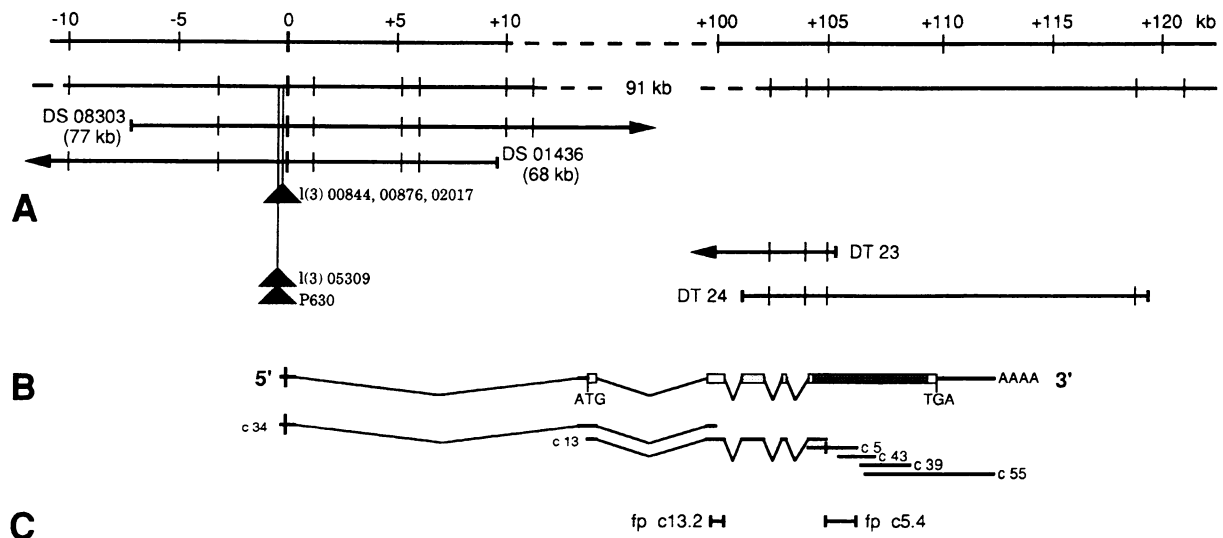


Fig. 1. Schematic representation of the cloned genomic region from 79E_{1,2}. (A) Approximately 130 kb of cloned DNA from the 79E_{1,2} chromosomal region are presented along with the *EcoRI* restriction sites. The *EcoRI* site at the extreme 5'-end of the cDNA, which is common to the cDNA and the genomic DNA, is arbitrarily chosen as position 0. The location of individual DNA alterations associated with P-element insertions is displayed below the genomic DNA. (B) Exon-intron structure of the *ten^m* gene. Five introns were identified either by sequencing genomic clones, or solely by cross-hybridization of the cDNAs with the genomic region and comparison of the restriction sites of the genomic region with the cDNAs. Note that the EGF-like region (light shaded region) and the region harbouring FN III repeats (dark shaded region) are encoded in one exon each. (C) Two different cDNA fragments which were expressed in bacteria and used to raise antibodies. A monoclonal antibody against an epitope from fp c13.2 (mAb 113) was used for the immunohistochemistry and immunoprecipitation experiments; polyclonal antisera against fp c13.2 and c5.4 were used in immunoprecipitation experiments and Western analysis.

the domain are also conserved, such as valines, asparagines, serines and glycines (consensus Figure 2B). These residues, however, do not conform to the set of more tightly conserved amino acids found in FN III repeats (Bork and Doolittle, 1993), suggesting that they may represent a diverged class of FN III repeats.

In contrast to vertebrate tenascin, a stretch of 112 amino acids (residues 558–669) is found separating the series of EGF-like repeats and the series of FN III repeats. These 112 amino acids, termed the 'CC' domain (Figure 2C), show a remarkably high degree of homology to the C-terminal domain of Ten^a (53% identity or 68% similarity;



Fig. 2. Open reading frame within the *ten^m* gene and alignment of related sequences. (A) Overlapping cDNA clones were isolated and sequenced to produce a 7545 bp open reading frame, which encodes the 2515 amino acid shown here. The putative signal peptide (1–38) is italicized. Potential glycosaminoglycan (GAG) attachment sites are in bold. A region representing two adjacent potential heparin binding sites that both conform to the heparin binding consensus (Cardin and Weintraub, 1989) is underlined. The position of the RGD tripeptide is indicated by smaller capital letters. (B) Alignment of the *Ten^m* sequence in groups of related motifs. All cysteine residues of the EGF-like domain are highlighted and the tyrosine and phenylalanine each replacing one of the cysteine residues are underlined. The identification of FN III-like repeats is based on the presence of conserved tryptophans and tyrosines (bold) and the ability to form β -sheets, based on secondary structure prediction programs (Devereux et al., 1984). A consensus is indicated at the bottom of each group of repeats and is based on the presence of a specific amino acid at a given position within at least six of the 11 repeats. (C) Different symbols for the various structural features were used to draw a model of *Ten^m*. At the N-terminus, the only hydrophobic sequence of the molecule was assigned to the signal peptide (SP). Eight EGF-like domains are indicated by diamonds. A shaded box termed 'CC' denotes a 110 amino acid cysteine-rich domain highly related to a domain shared with *Ten^a* (Baumgartner and Chiquet-Ehrismann, 1993). The boxes numbered 1–11 correspond to the FN III-like repeats. RGD, position of the RGD motif; N, potential N-linked glycosylation site; SG, potential glycosaminoglycan attachment site. Neither heptad repeat structures nor any potential cysteine residues were found in the N-terminus that could assemble one subunit into a multimeric protein. (D) Hydropathy plots using the algorithm of Kyte and Doolittle (Devereux et al., 1984), drawn in scale with the alignment in C). The only clear hydrophobic region is the signal peptide (SP).

Baumgartner and Chiquet-Ehrismann, 1993). Moreover, all cysteine residues are perfectly conserved within these two domains.

The last 277 amino acids do not display homology to fibrinogen as is found in tenascin; however, they show some local homologies to tenascin (amino acids 2352–2413, 33% identity or 57% similarity over 59 amino acids of the fibrinogen domain of chicken tenascin). They contain an RGD site which was shown to bind PS2 integrin (S.Baumgartner, unpublished data). Furthermore, a portion that conforms to the heparin binding consensus sequence (amino acids 2410–2422; Cardin and Weintraub, 1989) was found in front of the RGD tripeptide, suggesting that *Ten^m* might interact with heparin and possibly other glycosaminoglycans.

A database search has revealed a *Caenorhabditis elegans* gene, termed R13F6.4 (Wilson, 1994), whose gene product shows 29% identity to *Ten^m* over the entire length of 2531 amino acids. Thus, this gene is considered the *C.elegans* homologue of *ten^m*, in particular because the *ten^m* domain structure has also been shown to be conserved.

Western analysis and immunoprecipitation experiments indicate that *Ten^m* is a large secreted proteoglycan with an estimated molecular weight of 900–1000 kDa (Figure 3B, lanes a–f). The attached carbohydrate moiety is most likely composed of chondroitin sulfate or dermatan sulfate, because these chains are sensitive to chondroitinase ABC digestion (Figure 3B, lane f). The digestion releases a core of ~270 kDa (Figure 3B, lane f) which is in good agreement with the calculated molecular weight of 281 kDa deduced from the primary amino acid sequence.

Temporal and spatial distribution of *ten^m* transcripts

On Northern blots, probes containing a mixture of overlapping cDNAs detect two differentially regulated RNA species of 10.5 and 11.5 kb (Figure 3A). All developmental stages analysed show the 11.5 kb transcript. In contrast, the less abundant 10.5 kb transcript is observed only during early stages of embryogenesis (0–12 h). We do not have evidence for an alternatively spliced mRNA species within the coding region. Therefore, the smaller transcript probably arises from differential use of an alternative poly(A) addition signal that is located 800 bp upstream of the poly(A) addition signal of the major form of mRNA (data not shown).

Whole-mount *in situ* hybridization first detects *ten^m* transcripts during the 14th nuclear cycle, i.e. at stage 5. They are ubiquitously expressed along the anterior–posterior axis, except for a region on the dorsal side, where fewer transcripts are observed (Figure 4A, arrowheads), and at the anterior and posterior pole region where no transcripts are detected. Interestingly, *ten^m* transcripts are localized within cells at this stage and appear stippled in the basal portion of the apical periplasm (Figure 4A and B, arrows). Localized transcripts were also detected for *ten^a*, but not at identical positions within cells (Baumgartner and Chiquet-Ehrismann, 1993). The *ten^m* transcript pattern persists during early stages of germband extension (Figure 4D) until a repetitive pattern of 14 stripes appears in both the ectoderm and mesoderm (Figure 4E) which appear sharpened at stage 12

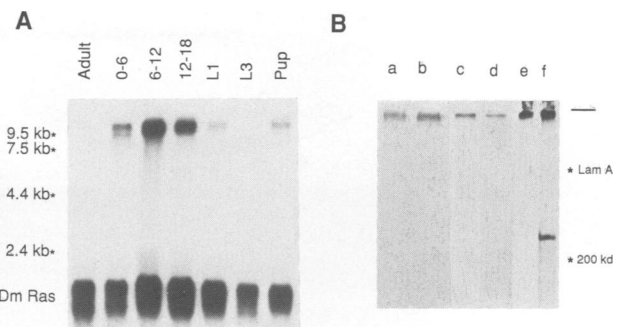


Fig. 3. (A) Northern blot analysis. Northern blot analysis of different stages throughout the *Drosophila* life cycle with a mixture of *ten^m* cDNAs (c13, c5 and c55). Each lane contains 5 µg of poly(A)⁺ RNA. The stage of the embryonic RNA is denoted in hours after egg laying; L1 and L3 are from the first- and third-instar larval stages, P from late pupal stages, and A from adult males and females. Two transcripts are detected which might derive from differentially polyadenylated mRNAs. The amount of loaded RNA was estimated by subsequent probing with a Dm Ras 64 probe (Mozer *et al.*, 1985). Transcript lengths were determined with a ladder of RNA standards (Bethesda Research Laboratories). (B) *Ten^m* is a large secreted proteoglycan containing chondroitin sulfate side chains. Lanes a and b: 5–13 h embryonic extracts were immunoprecipitated with (a) c5.4 antibodies and (b) c13.2 antibodies which precipitated a high molecular weight protein. Lanes c and d: 5–13 h embryonic extracts (c) and Schneider S2 conditioned medium (d) were immunoprecipitated by mab 113, followed by Western analysis using c5.4 antibodies; the same high molecular weight protein was detected. Lanes e and f: Schneider S2 cells were labelled in the presence of [³⁵S]methionine and the conditioned medium was immunoprecipitated using mab 113, split into a ratio of 1(e):2(f) and analysed without (e) or after (f) chondroitinase ABC digestion; the digestion, although not complete, releases a core of ~270 kDa. 5% polyacrylamide gels were run under reducing conditions for almost twice as long as it took for the dye front to reach the bottom of the gel. The line on the right above the size markers denotes the top end of the separation gel. Stars indicate positions of the mouse laminin A subunit (400 kDa) and of myosin (200 kDa).

(Figure 4F). Additional *ten^m* transcripts are seen in the presumptive cardiac cells and in the lymph gland (Figure 4F). After germband retraction (Figure 4G), *ten^m* expression is detected in cardiac cells, in the lymph gland and in the tracheal system. After head involution (Figure 4H and I), a dense pattern of stained neurons is observed in the ventral cord. In addition, ventro-lateral stripes corresponding to cells in the segmental furrows (arrow), a strong circumferential stripe in the cephalic region and single hemocytes reveal *ten^m* transcripts. At the time of hatching, transcripts are mainly confined to the ventral cord and to the brain (data not shown). During larval and pupal stages, *ten^m* transcripts are detected at low levels in the ventral cord, in the brain and in imaginal discs, but they appear stronger again in the developing eye during pupal stages (data not shown).

The expression of β-galactosidase from the enhancer trap line l(3) 05309 mentioned previously shows excellent overall agreement with the spatial expression of the *ten^m* mRNA at all embryonic stages (Figure 4C, J and K versus 4A, H and I).

The *Ten^m* protein is localized in seven stripes during the blastoderm stage

A series of monoclonal antibodies and two polyclonal antisera were raised against bacterial fusion proteins

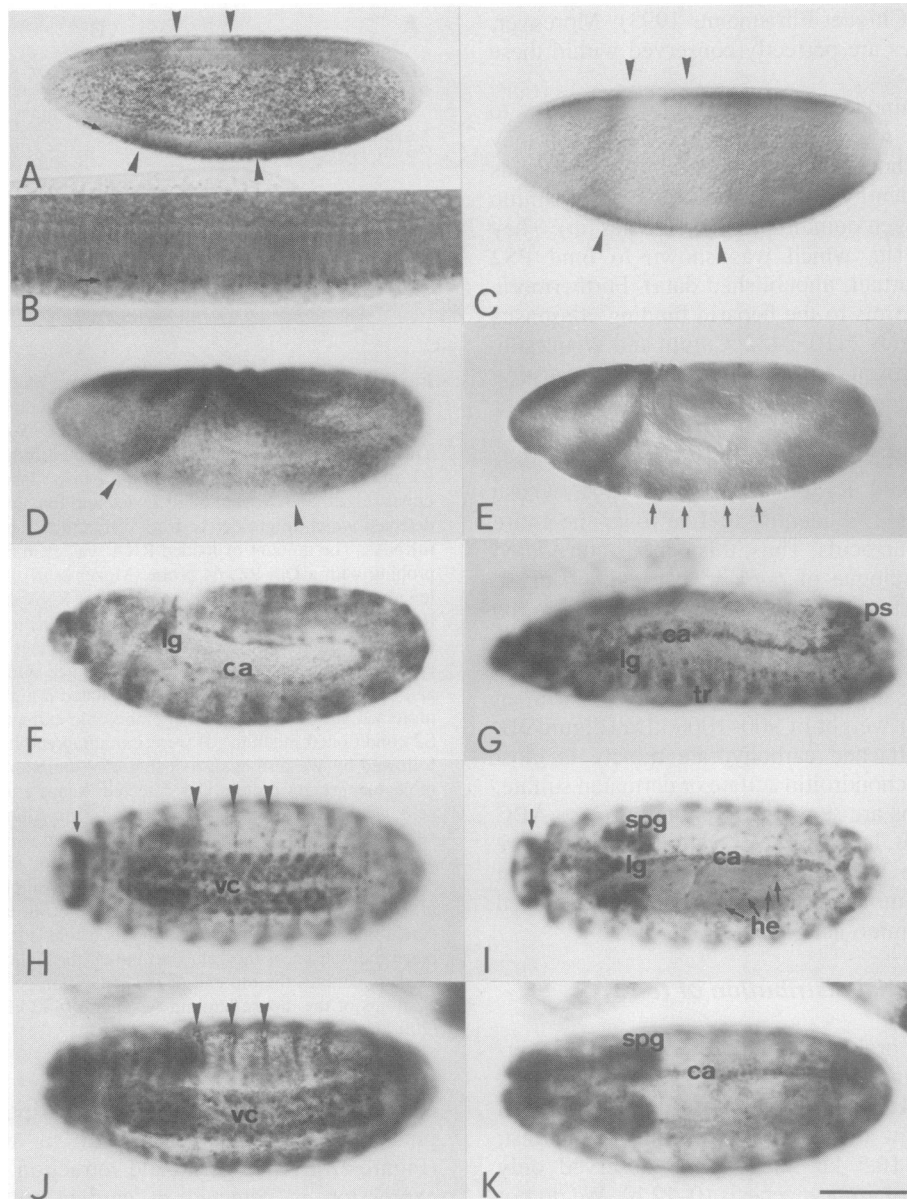


Fig. 4. Spatial expression of the *ten^m* gene and comparison with the LacZ pattern of the P-element line l(3) 05309. Whole-mount *in situ* hybridization (A, B and D–I) and LacZ staining (C, J and K). Embryos are oriented with anterior to the left and dorsal side up unless otherwise noted. [A and B (enlargement)]: stage 5 embryo (embryonic stages are those of Campos-Ortega and Hartenstein, 1985), mid-sagittal focal plane; the expression of *ten^m* is ubiquitous along the anterior–posterior axis, except for the regions at the anterior and posterior poles. Note a zone where fewer transcripts are detected (indicated by arrowheads) and a faint stripe at the location of the presumptive cephalic furrow (left arrowhead). *ten^m* transcripts are accumulated in the basal portion of the apical cytoplasm, immediately next to the nuclei (arrows in B). (C) Comparable LacZ staining of line l(3) 05309, same stage as in (A). (D) Stage 8 embryo; *ten^m* transcripts are still expressed uniformly with the exception of a region where fewer transcripts are detected (arrowheads). (E) Stage 10 embryo; a repetitive pattern becomes obvious (arrows). (F) Stage 12 embryo; 14 stripes emerge from the pattern seen in (E). Additional staining is observed in the lymph gland (lg) and cardiac cells (ca). (G) Stage 13 embryo after germband retraction; strong staining is seen in cardiac cells (ca), in the lymph gland (lg), in the posterior spiracles (ps) and in the tracheae (tr). (H) Ventral view and (I) corresponding dorsal view of the same embryo; *ten^m* transcripts are observed in the ventral cord (vc) and in the supraesophageal ganglia (spg), in the lymph gland (lg), in cardiac cells (ca), in hemocytes (he) and in a repetitive manner near the segmental furrows (indicated by arrowheads). (J and K) LacZ pattern of line l(3) 05309 equivalent to that shown in (H) and (I). Bar in (K) represents 100 μ m.

derived from specific portions of the Ten^m protein (Figure 1C), of which monoclonal antibody 113 was chosen for immunostaining of embryos.

Ten^m protein is first detected during cellularization of the blastoderm embryo (stage 5), and the protein pattern follows the *ten^m* mRNA pattern (Figure 5A). In addition to the mRNA pattern, an anterior domain (AD) of about eight cells in width is observed close to the anterior pole.

Posteriorly, the region between the pole cells and the terminal blastoderm nuclei shows strong Ten^m staining. Slightly later, a repetitive pattern evolves (Figure 5B) and at the time of cellular blastoderm, a pattern of seven circumferential stripes has arisen, each with a width of about four or five cells (Figures 5C and 6C). The stripe pattern is not absolutely regular because bands 1+2, 3+4 and 6+7 appear grouped. Anterior to stripe 1, a faint

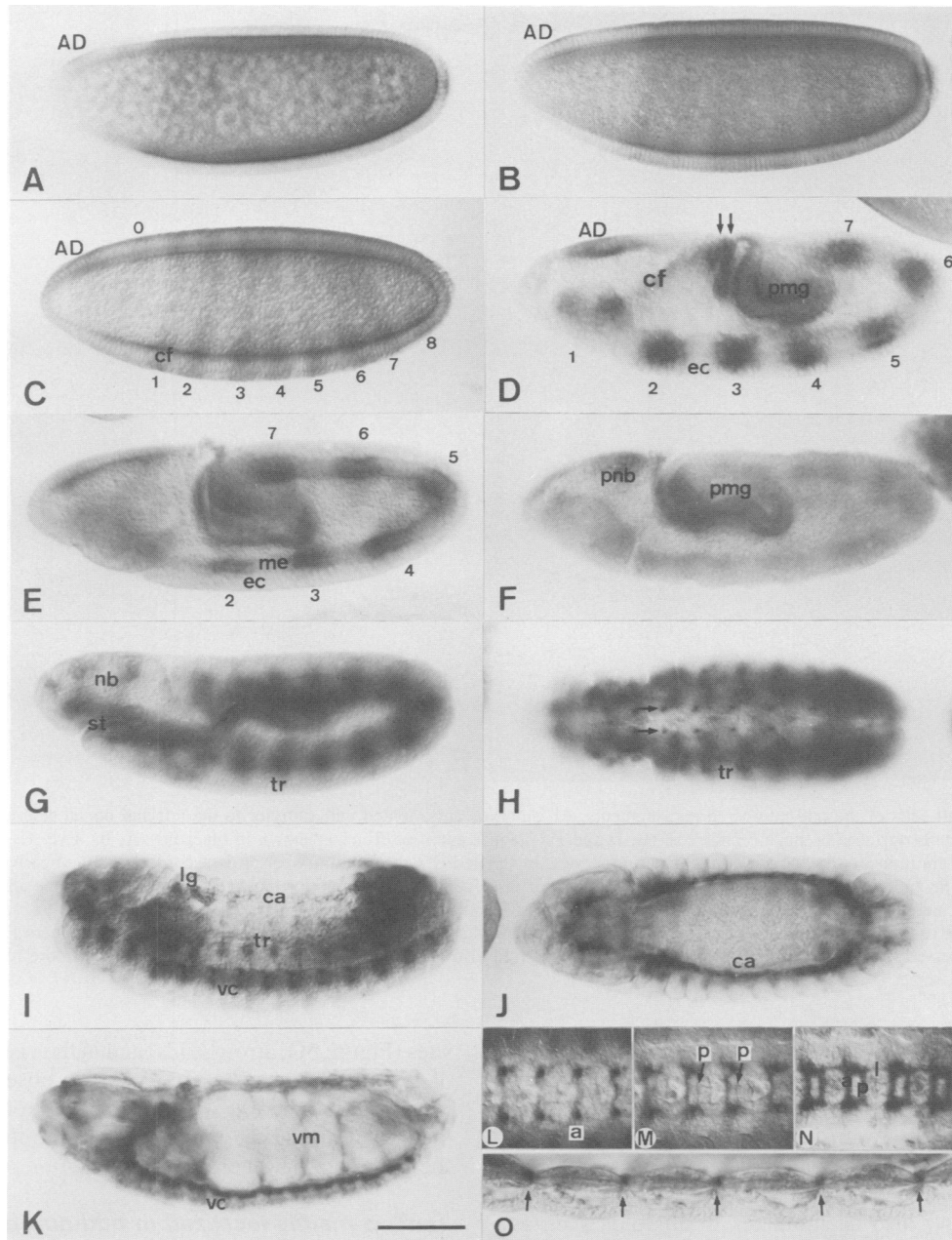


Fig. 5. Ten^m protein pattern during embryonic development. Embryos are oriented with anterior to the left and dorsal side up unless otherwise noted. (A) Stage 5 embryo (embryonic stages are as defined by Campos-Ortega and Hartenstein, 1985); Ten^m initially is expressed ubiquitously along the anterior–posterior axis and in a domain (anterior domain, AD) at the dorsal tip of the embryo. Note the accumulation of Ten^m at the cell wall which migrates inwards during cellularization. (B) Stage 5 embryo slightly older than that in (A); a repetitive pattern becomes obvious. (C) Stage 6 embryo; seven stripes have evolved. In addition, one partial stripe is seen on the dorsal side (stripe 0) and another partial stripe on the ventral side (stripe 8). (D) Stage 8 embryo; Ten^m is found in all furrows, i.e. in anterior and posterior transverse furrows (arrows), and in the posterior midgut (pmg). Note the decrease of Ten^m in the ectoderm (ec). (E) Stage 9 embryo; Ten^m is exclusively expressed in the mesoderm (me). (F) Stage 10 embryo; the repetitive pattern appears strongly reduced. Some neuroblasts of the procephalic lobe (pnb) show Ten^m . (G) Stage 11 embryo; a new pattern of expression in the developing tracheal system (tr) becomes apparent. Cells at the bottom of the stomodaeal (st) invagination begin to accumulate Ten^m . (H) Stage 12 embryo (ventral view); staining is observed in the developing tracheal system (tr) and on cell bodies of certain neurons (arrowheads). (I) Stage 13 embryo; Ten^m is on axons of the ventral nerve cord (vc), in cardiac cells (ca) and in the primordia of the lymph gland (lg). (J) Top view, slightly older embryo than in (I); strong staining is observed in cardiac cells (ca). (K) Stage 15 embryo; Ten^m is on axons of the ventral cord (vc) and in the visceral mesoderm of the midgut (vm). (L–N) High magnification of the ventral nerve cord of embryos during stages 12–15 denoting Ten^m during different stages of axonogenesis. Note that Ten^m initially stains the pioneering axons of the anterior (a) commissures, followed by the appearance on the pioneering axons of the posterior (p) commissures and the longitudinal (l) connectives. (O) High magnification of a stage 16 embryo showing staining on muscle attachment sites. cf, cephalic furrow. Bar in (K) corresponds to 100 μ m.

stripe 0 is visible only dorsally, while posterior to stripe 7 a weak stripe 8 is seen only ventrally. We interpret this pattern as the binding of Ten^m protein to a receptor that

is itself expressed in stripes. Since at this stage the RNA and protein patterns do not coincide, Ten^m is thought to be secreted both into the yolk and the perivitelline space,

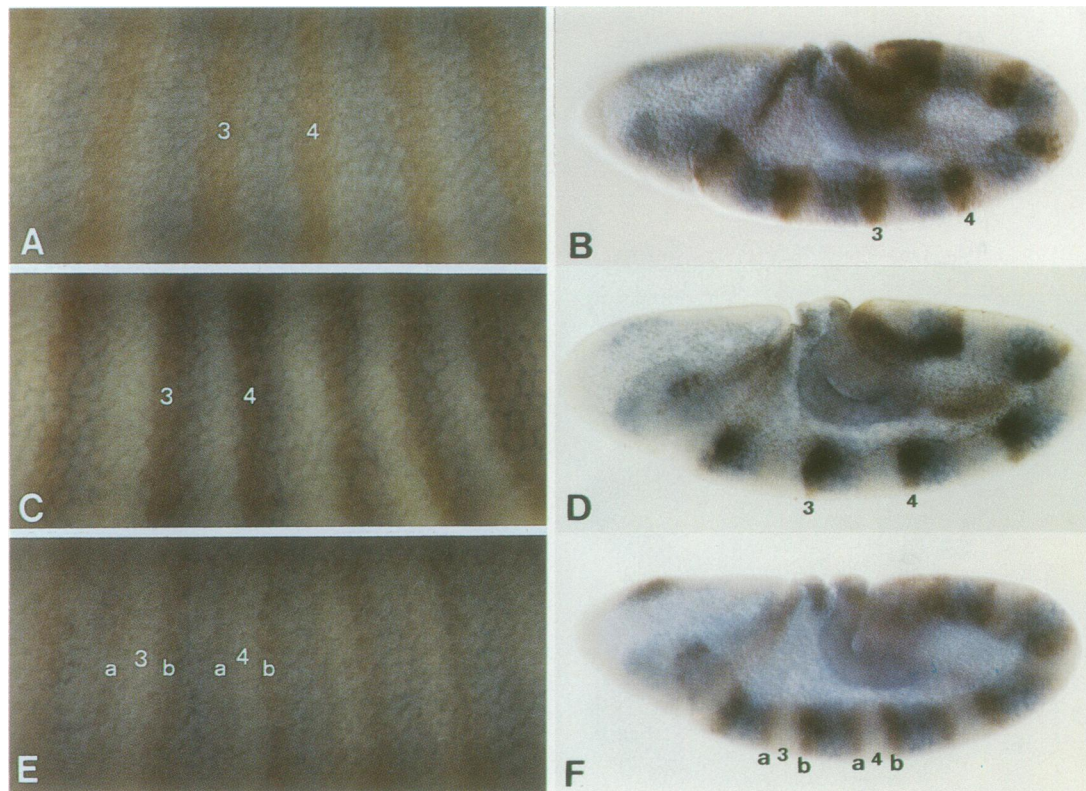


Fig. 6. Ten^m is on all cells of the odd-numbered parasegments. All embryos are oriented with anterior to the left and dorsal side up. (A, C and E): magnifications of lateral surfaces of stage 5 embryos. (B, D and F): stage 8 embryos. Ten^m is shown in blue; Ftz (A, B), Eve (C, D) and Prd (E, F) are in brown. Numbers indicate the corresponding pair-rule stripes. In (E) and (F), the band numbering is according to Baumgartner and Noll (1990). In (A) and (C), the *ftz* and *eve* stripes have narrowed down to two or three cells with the anterior-most cell coincident with the anterior borders of the parasegments (Lawrence *et al.*, 1987). Due to the irregularities of the *ten^m* stripes, Ten^m is not always in perfect register to Ftz or Eve (Figure 7C). In most cases, however, the anterior-most cell where Ten^m is detectable coincides with the anterior-most cell where Eve is detectable; hence, Ten^m is expressed in cells of the odd-numbered parasegments (see also Figure 9). Note that the *ten^m* stripes appear more regular during germband extension stages (Figure 7B, D and F).

and to diffuse laterally until it can bind to its receptor. We cannot exclude other possibilities, such as differential translation of the *ten^m* RNA.

During germband extension the stripes appear more regular and Ten^m is more strongly detected on surfaces of mesodermal and ectodermal cells and the ECM in between (Figure 5D). Ten^m also accumulates in all folds such as the cephalic furrow, anterior and posterior transverse fold and the posterior midgut plate. During progressing germband extension (Figure 5E) Ten^m becomes restricted to the mesoderm, and at the extended germband stage the stripes have vanished almost completely (Figure 5F). Residual Ten^m is observed only in procephalic neuroblasts and in the posterior midgut. Later, at stage 11 (Figure 5G), Ten^m is found in the tracheal system and in the stomodeum. During the first stages of axonogenesis (stage 12/3, Klämbt *et al.*, 1991), Ten^m staining is on cell bodies of a subset of neurons (arrowheads in Figure 5H) and on the developing tracheal system.

After germband retraction (Figure 5I–O), prominent staining is seen on pioneering axons of the anterior commissures (Figure 5H and L), and later on axons of the posterior commissures (Figure 5M) and on longitudinal connectives (Figure 5N). Strong staining is also observed on cardiac cells and lymph glands (Figure 5I and J), on the tracheal system (Figure 5I), around muscle attachment

sites (Figure 5O, arrowheads) and in the visceral mesoderm of the gut (Figure 5K). Ten^m is also observed during all larval stages where it is expressed on axons and imaginal discs, and during the pupal stage where it is expressed in the eye (data not shown).

Ten^m is mainly localized in odd-numbered parasegments

To determine the phase of the Ten^m stripes relative to the stripes of pair-rule genes, we examined embryos at the stage of cellular blastoderm (stage 5) and germband extension (stage 8) using the monoclonal antibody 113 for Ten^m staining and polyclonal rabbit antisera against the Ftz, Eve and Prd proteins (Frasch and Levine, 1987; Krause *et al.*, 1988; Gutjahr *et al.*, 1993). It is noteworthy that neither the width nor the spacing of the Ten^m bands is completely regular as compared with the Ftz and Eve patterns. As shown in Figure 6A and B, Ten^m and Ftz appear as alternating bands which do not overlap. Ftz is expressed in two or three cells at that stage and leaves a gap of about one or two cells expressing neither Ftz nor Ten^m . Conversely, Ten^m is found in perfect register to Eve in most cases (Figure 6C and D). Since the anterior borders of Ftz and Eve are coincident with the anterior borders of the parasegments (Lawrence *et al.*, 1987), we conclude that Ten^m is expressed in all odd-numbered parasegments

(Figure 9). With regard to Prd, *Ten^m* covers the anterior cell of all 'a' bands of Prd and the posterior cell of all 'b' bands of Prd (Figures 6E and F, and 9).

ten^m mutants exhibit a pair-rule phenotype

In search for mutations at the *ten^m* locus, four enhancer trap lines (Karpen and Spradling, 1992) and one P-element line (Cooley *et al.*, 1988) were obtained that all had a P-element inserted at 79E_{1,2} (Figure 1A). All five lines were subjected to molecular analysis of the integration site of the P-element. Plasmid rescue in combination with sequencing of the genomic region showed that all alleles had P-element insertions within 70 bp of the extreme 5'-end of the transcript (Figure 1A). Since l(3) 00844, 00876 and 02017 turned out to be identical alleles, three independent lethal *ten^m* alleles were identified. l(3) 02017 and 05309 were also analysed for their enhancer trap expression pattern and were found to exhibit a *LacZ* pattern comparable with the endogenous *ten^m* mRNA pattern (Figure 4C, J and K).

To assess the function of *ten^m* during development,

cuticle preparations of homozygous lethal embryos derived from all three alleles were examined. l(3) 02017 exhibits a cuticular phenotype indistinguishable from wild-type larvae (Figure 7A). P630 displays a weak phenotype in that, in most cases, an incomplete fusion of ventral denticle belts of the fourth and fifth abdominal segment (A4 and A5) was observed (Figure 7B). Fusions of A6 and A7, or A2 and A3, were observed at the same frequency (data not shown). Additional fusions of A2+A3 and A4+A5 were observed, but at a lower frequency (Figure 7C). The l(3) 05309 allele showed the cuticular pattern most severely affected (Figure 7D–F). This line shows a range of phenotypic severity with partial fusion (Figure 7D), nearly complete (Figure 7E) and complete fusion of adjacent denticle belts (Figure 7F), indicative of an *opa*-like phenotype. The *opa* phenotype is characterized by deletions of denticle belts of T2, A1, A3, A5 and A7 and naked cuticle of T1, T3, A2, A4 and A6 (Jürgens *et al.*, 1984). A weak and a strong *opa* allele were chosen for comparison with the *ten^m* phenotype. The weak allele, *opa^{13D92}*, exhibits a similar phenotypic series of partial fusions of denticle

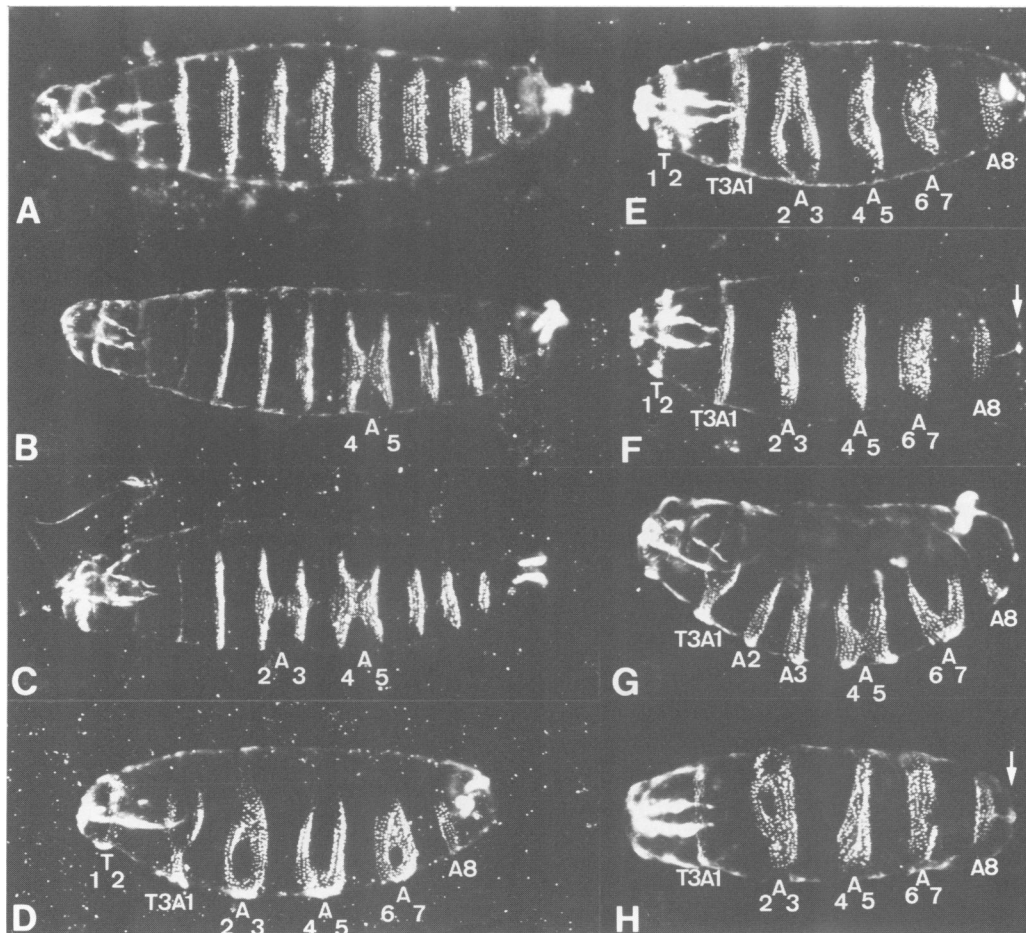


Fig. 7. Phenotype of *ten^m* lethal mutations leading to an *odd-paired*-like phenotype. Cuticular preparations of an allelic series of embryos just prior to hatching. (A) Homozygous or heterozygous l(3) 02017 embryo which is indistinguishable from wild-type larvae. (B and C) Homozygous P630 embryos. A pairwise fusion of A4+A5 is observed in B or adjacent pairwise fusions of A2+A3 and A4+A5 in C. (D–F) Homozygous l(3) 05309 embryos. Pairwise fusion of adjacent segments occurs in each case. The fusions are least complete in D and most complete in F. (G) Weak *opa^{13D92}* allele and (H) strong *opa^{11P32}* allele. Note the incomplete pairwise fusion in a weak *opa* allele similar to D and the complete pairwise fusion of a strong *opa* allele similar to E. Arrows in F and H indicate the absence of portions of the telson (Jürgens, 1987). Note that the difference in the phenotypes between P630 and l(3) 05309 is only caused by the insertion of different types of P-element constructs (P[PZ] versus P[neo^R]), because both P-element insertions are at identical nucleotide positions (Figure 1A).

belts (Figure 7G versus D) whereas the strong allele, *opa*^{HP32}, is virtually indistinguishable from a strong *ten*^m allele (Figure 7H versus E).

ten^m is a secondary pair-rule gene

To address the question of where *ten*^m is located within the hierarchy of pair-rule genes, we examined the *Ten*^m pattern in several pair-rule and segment-polarity mutant backgrounds, as well as examining other pair-rule and segment-polarity gene expression patterns in a *Ten*^m mutant background. In *fiz*⁻ embryos, the initial wild-type *ten*^m pattern (Figure 5A) is maintained through the blastoderm

and germband extension stages (Figure 8C and D) and no striped pattern appears. Conversely, in *eve*⁻ embryos, while the initial wild-type pattern of continuous expression and subsequent refinement into stripes occurs normally (data not shown), all *Ten*^m stripes except stripes 3 and 4 virtually disappear during the early gastrula stage (Figure 8E). These two bands almost disappear later during germband extension (Figure 8F). In contrast to the protein pattern, the *ten*^m mRNA pattern is affected in neither *ftz* nor *eve* mutant backgrounds at stage 5 (data not shown), indicating that these pair-rule genes control the *Ten*^m protein localization, and not *ten*^m transcription. No changes

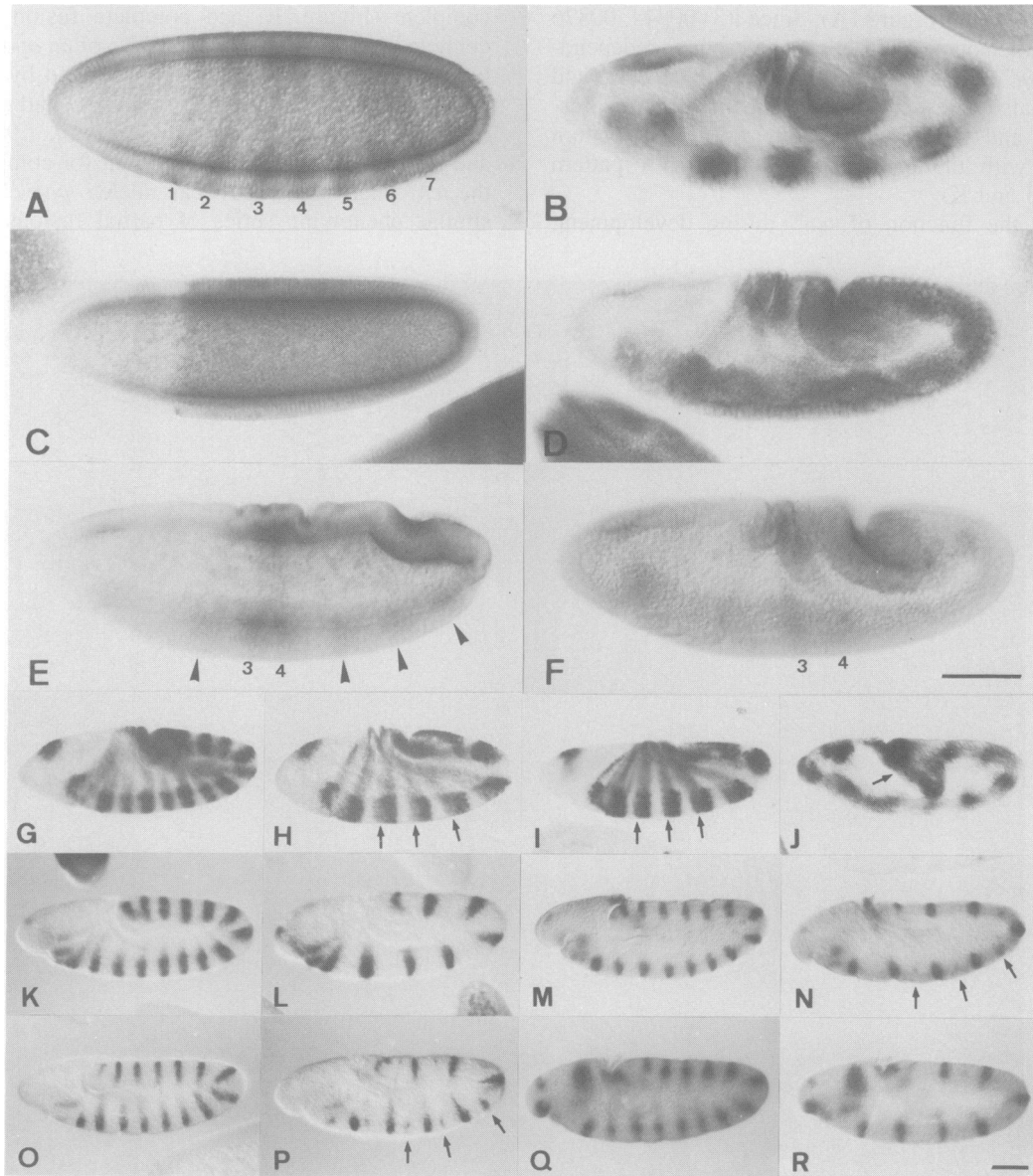


Fig. 8. *ten*^m acts within the hierarchy of pair-rule genes. All embryos are oriented with anterior to the left and dorsal side up. (A and B) *ten*^m staining in wild-type stage 6 (A) and stage 8 (B) embryos. (C and D) *ten*^m staining in homozygous *ftz*^{w20} stage 6 (C) and stage 8 (D) embryos. (E) and (F) *ten*^m staining in homozygous *eve*^{R13} stage 7 (E) and stage 8 (F) embryos. Arrowheads show remnants of stripes 2, 5, 6 and 7. (G–I) *prd* staining in wild-type stage 8 embryos (G), homozygous *l(3) 05309* stage 8 embryos (H) and homozygous *opa*^{HP32} stage 8 embryos (I). Note that the *prd* patterns in (H) and (I) are identical. (J) *ten*^m staining in *opa*^{HP32} stage 9 embryos virtually showing a wild-type pattern. *opa*⁻ embryos can be identified unambiguously at this stage because they show an abnormally oblique posterior midgut invagination (arrow). (K–R) Expression of *slp1* (K and L), *gsb* (M and N), *en* (O and P) and *wg* (Q and R) in wild-type embryos at the germband extension stage (K, M, O and Q) and homozygous *l(3) 05309* mutant embryos of the same stage (L, N, P and R). All patterns analysed show half the number of bands in a *ten*^m mutant background, with the exception of *gsb* (N) and *en* (P), where vestiges of even-numbered bands appear in the mesoderm (arrows). The bars in (F) and (R) correspond to 100 μ m.

in the Ten^m pattern were observed in *opa* (Figure 8J), *prd* and *slp* mutant embryos (data not shown).

A number of antisera against pair-rule proteins (Ftz, Eve and Prd) and segment-polarity proteins (Slp1, Gsb, En and Wg) were used to analyse the corresponding patterns in the strongest *ten^m* mutant background, I(3) 05309. Of the pair-rule genes, the *ftz* and *eve* patterns did not show any alterations in a *ten^m* mutant background (data not shown). In contrast, the *prd* pattern is dramatically altered. Instead of 14 wild-type stripes (Figure 8G), seven broad bands were observed with the anterior half fading out during gastrulation (Figure 8H, arrows). Since the evolution of the *prd* pattern in (H) was strongly reminiscent of the previously reported *prd* pattern in *opa* mutants (Baumgartner and Noll, 1990), the analysis was repeated, confirming that the *prd* pattern in *ten^m* and *opa* mutants is identical (Figure 8H versus I). Moreover, since the *ten^m* pattern was not altered in *opa* mutants (Figure 8J), we conclude that either *ten^m* and *opa* can act independently on *prd*, or *ten^m* acts upstream of *opa*.

The *slp1* pattern and all segment-polarity gene patterns analysed show half the number of stripes missing in *ten^m* mutants (Figure 8L, N, P and R), indicating that *ten^m* is needed to activate one set of stripes of *slp1*, *gsb*, *en* and *wg*. In the case of *gsb* and *en*, vestiges of the elsewhere missing stripes were observed (Figure 8N and P), in particular in the mesoderm. Such vestiges of *gsb* and *en* bands were also observed in an *opa* mutant background by others (DiNardo and O'Farrell, 1987; Baumgartner, 1988) suggesting that *ten^m* and *opa* exert a similar control function on *gsb* and *en* expression.

Discussion

The *ten^m* gene encodes a secreted protein which likely participates in a signal transduction cascade

Our data indicate that *ten^m* encodes a large ECM protein with glycosaminoglycan side chains attached to the Ten^m core. Ten^m was shown to harbour several different domains, a characteristic feature of ECM proteins. It contains tenascin-type EGF-like repeats and FN III-like domains, but in contrast to vertebrate tenascin, it lacks the fibrinogen domain. Moreover, glycosaminoglycan side chains are attached which do not appear in the vertebrate counterpart.

We have shown that Ten^m is a secreted protein. The discrepancy between the *ten^m* RNA and protein patterns might be explained by the existence of a receptor which is expressed in stripes. Alternatively, we cannot exclude mechanisms involving differential translation, post-translational modifications or stabilization. Our results suggest that the proposed receptor mediates the extracellular action of Ten^m into the nucleus via a signal transduction cascade. Hence, it is tempting to speculate that at least one other locus exists which can lead to a pair-rule phenotype similar or identical to *opa*. Genes further downstream from *ten^m* and its receptor may also encode ubiquitous cellular factors which might not lead to a pair-rule phenotype.

The size of the *ten^m* gene limits its expression during early cleavage stages

Apart from the proposed mode of action, the *ten^m* gene is also unique among segmentation genes with respect to

its size which exceeds 110 kb (Figure 1). Taking into account the very long time taken to synthesize the *ten^m* primary transcript (>80 min; based on data from Shermoen and O'Farrell, 1991), it is plausible that the synthesis of the *ten^m* transcript begins only during cell cycle 14, because all earlier cell cycles are much shorter and transcription of all genes is interrupted during mitosis (Prescott and Bender, 1962). However, cycle 14 is still not long enough to complete the synthesis of all *ten^m* transcripts and, consequently, many of the transcripts that are initiated will be aborted and the yield of completed transcripts will depend on both the timing during the cell cycle at which transcription is initiated and the length of the cycle. Consequently, abortion of transcription may modify the spatial pattern and level of accumulation of *ten^m* transcripts. Never during this time period, however, could we detect the *ten^m* RNA in stripes, even though 3'-*ten^m* cDNA probes were used which would exclusively detect completed transcripts (data not shown). Since the *ten^m* RNA is found to be localized within cells at that stage (Figure 4B), we hypothesize that, following synthesis, the *ten^m* RNA is trapped by an RNA-localizing system, as was shown to exist for *ten^a* (Baumgartner and Chiquet-Ehrismann, 1993).

***ten^m* may modulate the activity of Opa protein**

Comparison of the *ten^m* and the *opa* mutant phenotypes indicates the possibility of an epistatic relationship between these two genes. This hypothesis is strengthened by the observation that the *prd*, *gsb* and *slp1* patterns are identical in both mutants (Figure 8H and I; Baumgartner, 1988; Grossniklaus, 1993; Li *et al.*, 1993), while the *ten^m* pattern remains virtually unaffected in *opa* mutants (Figure 8J). These findings indicate that *ten^m* probably acts upstream of *opa*. Benedyk *et al.* (1994) showed that Opa is not expressed in stripes, instead, it is found throughout all segment primordia. In fact, they argued that Opa is probably active in all cells and suggested that Opa function may vary in the presence of other transcription factors. Accordingly, we propose that Opa function might be modified by an inductive signal that alters its state of activity. Therefore, although the Opa protein is expressed throughout all segment primordia, the activity of the Opa protein may show a striped pattern (Figure 9). In this context, it seems unlikely that Ten^m controls the transcription of *opa*, because *opa* transcripts appear earlier than the Ten^m protein during cycle 14.

On the other hand, it is also conceivable that *ten^m* and *opa* act independently. In this case, Ten^m is expected to induce a downstream factor which may act, in concert with Opa, on downstream genes such as *prd* or *slp*.

***ten^m* and the regulatory network with other segmentation genes**

Our experiments clearly demonstrate that *ten^m* is dependent on *ftz* and *eve*, while *prd*, *slp1*, *gsb*, *en* and *wg* rely on the *ten^m* function (Figure 8), suggesting that *ten^m* is a secondary pair-rule gene.

Our results suggest that *prd* is a likely downstream target of the *ten^m*-induced signalling cascade. All 'a' bands of *prd* that straddle the boundaries of the odd-/even-numbered parasegments fade out, just after the *ten^m* stripes have been established and the proposed signal transduction

of germband extension. *ten^m* mutants, however, show an almost normal rate of germband extension (Figure 8L, N, P and R), most likely due to the fact that the strongest *ten^m* allele, l(3) 05309, is not a protein-null allele (data not shown). Possibly, other systems that confer selective adhesion proposed in the model are still active in a *ten^m* mutant, suggesting that a primary pair-rule gene such as *eve* is needed to inhibit these proposed functions which ultimately lead to an embryo with defective germband extension (Figure 8F). Strikingly, *Ten^m* is also absent in *eve* mutant embryos (Figure 8F), which correlates well with the above model.

One further coincidence is the position of the *ten^m* stripes with respect to the position of all folds occurring during gastrulation: Stripe 1 is exactly within the cephalic furrow (Figure 5C and D), while stripes 2 and 5 are within the anterior and posterior transverse furrows (Figure 5D). Furthermore, *Ten^m* is also found in the posterior midgut plate (Figure 5D), suggesting that perhaps the positions of events where cell movements take place are spatially determined through *Ten^m*, which may act in cooperativity with the cell movements leading to the process of germband extension.

Materials and methods

Fly stocks

All *ten^m* alleles [P630, l(3) 00844, 00876, 02017 and 05309] were obtained in two screens for P-element insertion lines (Cooley *et al.*, 1988; Karpen and Spradling, 1992). We performed a complementation analysis for lethality between the insertion lines as a matrix of each line against the rest of the alleles. These crosses confirmed that all insertion lines are allelic for the *ten^m* mutation. Trans-allelic combinations of all three *ten^m* alleles show the same series of phenotypes; however, in most cases the phenotype falls towards the phenotype of the less severe allele of the pair (data not shown). To generate revertants of l(3) 05309, 02017 and P630, P[PZ] and [P-neo^R] were mobilized with the endogenous $\Delta 2$ -3 transposase (Robertson *et al.*, 1988) and several non-lethal revertant lines of each allele were obtained and checked by Southern analysis and PCR to likely represent perfect P-excisions. The cuticular phenotype of these revertants was indistinguishable from wild-type. Other pair-rule alleles used in this study were *ftz^{w20}*, *eve^{R13}*, *prd^{2.45.17}*, *opa^{13D92}*, *opa^{IIP32}* and *slp^{A66C}*.

DNA and RNA techniques

Southern and Northern blot analyses were performed by standard procedures (Maniatis *et al.*, 1982). Hybridization at reduced stringency was carried out essentially according to McGinnis *et al.* (1984). RNA was extracted by the guanidium thiocyanate/phenol/chloroform extraction method of Chomczynski and Sacchi (1987). Poly(A)⁺ RNA was isolated using a Pharmacia Kit (Pharmacia).

Isolation of genomic and cDNA clones

Low stringency hybridization with a fragment from the EGF-like repeats of chicken tenascin indicated the presence of several cross-hybridizing loci in the *Drosophila* genome (Baumgartner and Chiquet-Ehrismann, 1993). Since a common 20 kb *EcoRI* band was detected independently using the initial 760 bp PCR fragment of *ten^a* (Baumgartner and Chiquet-Ehrismann, 1993), which also harbours tenascin-type EGF-like repeats, we probed a Df (2R) *Sb1/CyO* library (Baumgartner *et al.*, 1987) with the 760 bp PCR fragment of *ten^a* under low stringency conditions (McGinnis *et al.*, 1984). Several phage clones were recovered. One of the terminal *EcoRI* fragments of DT 24 contained the cross-hybridizing sequences and was sequenced; this confirmed the presence of additional tenascin-type EGF-like sequences in the *Drosophila* genome. This genomic *EcoRI* fragment was used to screen a randomly primed 0–16 h cDNA library, yielding several overlapping cDNA clones. Fragments from both the 5' and 3' ends of c13 were used to rescreen a randomly primed 0–16 h cDNA library, as well as an additional 8–12 h cDNA library (Brown and Kafatos, 1988). Through several reiterative rounds of sequencing, mapping and rescreening, a series of overlapping

cDNA clones comprising 11.4 kb in length was obtained (Figure 1B). These span almost the full length of the 11.5 kb mRNA that was predicted from Northern blot analysis (Figure 3A). P1 phages and a walk using phages from the Df (2R) *Sb1/CyO* library were used to clone the genomic region between exons 1 and 3 (Figure 1).

Sequencing

Genomic fragments and cDNAs were subcloned into the Bluescript vector (Stratagene). Both strands were sequenced using a Sequenase kit (US Biochemicals) and a nested deletion kit (Pharmacia).

Whole-mount *in situ* hybridization

Whole-mount *in situ* hybridizations were conducted using digoxigenin-labelled cDNAs from c13, c5 and c55 (Figure 1B) following the protocol of Tautz and Pfeiffle (1989).

Generation of antibodies and embryo staining

As indicated in Figure 1C, portions of two cDNA clones were cloned into the appropriate pGEX expression vectors (Pharmacia). After induction and lysis of cells, fusion proteins were extracted in a series of increasing urea concentration (Wingender *et al.*, 1989). Fusion proteins c13.2 and c5.4 correspond to amino acids 56–251 and 912–1391 respectively of the *ten^m* sequence. The fusion proteins were used to generate monoclonal antibodies and rabbit polyclonal antisera. Polyclonal antisera c13.2 and c5.4 were affinity purified over a corresponding β -galactosidase fusion protein column and eluted with 0.1 M glycine pH 2.5. For embryo staining, mab 113 was used at a dilution of 1:300 and rabbit anti- β -galactosidase antibodies (Cappel) were used at a dilution of 1:5000.

Immunoprecipitation and Western blotting

Samples of conditioned medium or immunoprecipitated extracts from 5–13 h embryos were separated by 5% SDS–PAGE. Following transfer onto nylon membranes, blots were probed with anti-*Ten^m* antibodies and detected with horseradish peroxidase conjugated secondary antibodies, followed by ECL chemiluminescence (Amersham). Detection of ³⁵S-labelled *Ten^m* protein in the medium was performed by metabolically labelling [0.1 mCi/ml Tran³⁵S-Label (ICN)] Schneider S2 cells for 24 h in M3 medium (minus methionine and cysteine), followed by immunoprecipitation of the conditioned medium with anti-*Ten^m* antibodies and protein A–Sepharose CL-4B (Pharmacia). Precipitates were washed twice with TNE (20 mM Tris–HCl pH 7.2, 150 mM NaCl, 1 mM EDTA, 0.5% NP40) and once with water, followed by separation by SDS–PAGE and autoradiography. Chondroitinase ABC digestion was performed using 5 U/40 μ l Sepharose beads; precipitates were digested for 3 h at 37°C.

EMBL accession number

The accession number for the *ten^m* cDNA sequence is X73154.

Acknowledgements

We are especially grateful to Dr Allan Spradling and his laboratory for the isolation of the *ten^m* mutants, and to the *Drosophila* Genome Center and the Bloomington Stock Center for providing us with the appropriate stocks and P1 phages. We thank the Gehring lab for providing fly stocks and for *ftz*, *eve*, *slp1* and *en* antibodies, Markus Noll for providing libraries and Prd and Gsb antibodies, and the Nusse lab for *wg* antibodies. We wish to thank Ken Irvine for discussions on germband extension and Martin Baron for help in the analysis of fibronectin type III repeats. We would like to thank Markus Noll, Liam Keegan, Markus Affolter, Ken Irvine and Tony Raizis for comments on the manuscripts. The secretarial help of Luigina Beffa is warmly acknowledged.

References

- Aukhil, I., Joshi, P., Yan, Y. and Erickson, H.P. (1993) *J. Biol. Chem.*, **268**, 2542–2553.
- Baumgartner, S. (1988) *Patterns of paired and gooseberry transcripts in wild-type and segmentation mutant embryos imply a combinatorial regulation of segmentation genes in Drosophila*. PhD thesis, University of Basel.
- Baumgartner, S. and Chiquet-Ehrismann, R. (1993) *Mech. Dev.*, **40**, 165–176.
- Baumgartner, S. and Noll, M. (1990) *Mech. Dev.*, **1**, 1–18.

- Baumgartner, S., Bopp, D., Burri, D. and Noll, M. (1987) *Genes Dev.*, **1**, 1247–1267.
- Benedyk, M.J., Mullen, J.R. and DiNardo, S. (1994) *Genes Dev.*, **8**, 105–117.
- Bopp, D., Jamet, E., Baumgartner, S., Burri, M. and Noll, M. (1989) *EMBO J.*, **8**, 3447–3457.
- Bork, P. and Doolittle, R. (1992) *Proc. Natl Acad. Sci. USA*, **89**, 8990–8994.
- Bristow, J., Tee, M.K., Gitelman, S.E., Melton, S.H. and Miller, W.L. (1993) *J. Cell Biol.*, **122**, 265–278.
- Brown, N.H. and Kafatos, F.C. (1988) *J. Mol. Biol.*, **203**, 425–437.
- Cadigan, K., Grossniklaus, U. and Gehring, W.J. (1994) *Genes Dev.*, **8**, 899–913.
- Campos-Ortega, J.A. and Hartenstein, V. (1985) *The Embryonic Development of Drosophila melanogaster*. Springer, Berlin.
- Cardin, A.D. and Weintraub, H. (1989) *Arteriosclerosis*, **9**, 21–32.
- Chiquet-Ehrismann, R. (1990) *FASEB J.*, **4**, 2598–2604.
- Chomczynski, P. and Sacchi, N. (1987) *Anal. Biochem.*, **162**, 156–159.
- Cooley, L., Kelley, R. and Spradling, A.C. (1988) *Science*, **239**, 1121–1128.
- Devereux, J., Haerberli, P. and Smithies, O. (1984) *Nucleic Acids Res.*, **12**, 387–396.
- DiNardo, S. and O'Farrell, P.H. (1987) *Genes Dev.*, **1**, 1212–1225.
- DiNardo, S., Sher, E., Heemskerk-Jongens, J., Kassis, J.A. and O'Farrell, P.O. (1988) *Nature*, **332**, 604–609.
- Erickson, H.P. (1993) *Curr. Opin. Cell Biol.*, **5**, 869–876.
- Erickson, H.P. and Bourdon, M.A. (1989) *Annu. Rev. Cell Biol.*, **5**, 71–92.
- Frasch, M. and Levine, M. (1987) *Genes Dev.*, **1**, 981–995.
- Gitelman, S.E., Bristow, J. and Miller, W.L. (1992) *Mol. Cell. Biol.*, **12**, 2124–2134.
- Grossniklaus, U. (1993) *Identification of developmentally regulated genes by enhancer detection: isolation and characterization of the Drosophila segmentation locus sloppy paired*. PhD thesis, University of Basel.
- Grossniklaus, U., Pearson, R.K. and Gehring, W.J. (1992) *Genes Dev.*, **6**, 1030–1051.
- Gutjahr, T., Frei, E. and Noll, M. (1993) *Development*, **117**, 609–623.
- Irvine, K.D. and Wieschaus, E. (1994) *Development*, **120**, 827–841.
- Jürgens, G. (1987) *Roux's Arch. Dev. Biol.*, **196**, 141–157.
- Jürgens, G., Wieschaus, E., Nüsslein-Volhard, C. and Kluding, H. (1984) *Roux's Arch. Dev. Biol.*, **193**, 283–295.
- Karpen, G.H. and Spradling, A.C. (1992) *Genetics*, **132**, 737–753.
- Klämbt, C., Jacobs, J.R. and Goodman, C.S. (1991) *Cell*, **64**, 801–815.
- Krause, H.M., Klemenz, R. and Gehring, W. (1988) *Genes Dev.*, **2**, 1021–1036.
- Lawrence, P.A., Johnston, P., Macdonald, P. and Struhl, G. (1987) *Nature*, **328**, 440–442.
- Li, X., Gutjahr, T. and Noll, M. (1993) *EMBO J.*, **12**, 1427–1436.
- Maniatis, T., Fritsch, E.F. and Sambrook, J. (1982) *Molecular Cloning: A Laboratory Manual*. Cold Spring Harbor Laboratory Press, Cold Spring Harbor, NY.
- Martinez-Arias, A., Baker, N.E. and Ingham, P.W. (1988) *Development*, **103**, 157–170.
- Matsumoto, K., Ishihara, N., Ando, A., Inoko, H. and Ikemura, T. (1992) *Immunogenetics*, **36**, 400–403.
- McGinnis, W., Hafen, E., Kuroiwa, A. and Gehring, W.J. (1984) *Nature*, **308**, 428–433.
- Mozer, B., Marlor, R., Parkhurst, S. and Corces, V. (1985) *Mol. Cell. Biol.*, **5**, 885–889.
- Nörenberg, U., Wille, H., Wolff, J.M., Frank, R. and Rathjen, F.G. (1992) *Neuron*, **8**, 849–863.
- Pearson, C.A., Pearson, D., Shibahara, S., Hofsteenge, J. and Chiquet-Ehrismann, R. (1988) *EMBO J.*, **7**, 2977–2982.
- Prescott, D. and Bender, M. (1962) *Exp. Cell Res.*, **26**, 260–268.
- Rathjen, F.G., Wolff, J.M. and Chiquet-Ehrismann, R. (1991) *Development*, **113**, 151–164.
- Robertson, H.M., Preston, C.R., Phillis, R.W., Johnson-Schlitz, D.M., Benz, W.K. and Engels, W. (1988) *Genetics*, **118**, 461–470.
- Saga, Y., Yagi, T., Ikawa, Y., Dakakura, T. and Aizawa, S. (1992) *Genes Dev.*, **6**, 1821–1831.
- Shermoen, A.W. and O'Farrell, P.O. (1991) *Cell*, **67**, 303–310.
- Spring, J., Beck, K. and Chiquet-Ehrismann, R. (1989) *Cell*, **59**, 325–334.
- Tautz, D. and Pfeiffle, C. (1989) *Chromosoma*, **98**, 81–85.
- Von Heijne, G. (1986) *Nucleic Acids Res.*, **14**, 4683–4690.
- Wieschaus, E., Sweeton, D. and Costa, M. (1991) In Keller, R., Clark, W.H. and Griffin, F. (eds), *Gastrulation: Movements, Patterns and Molecules*. Plenum Press, New York, pp. 213–224.
- Wilson, R. (1994) *Nature*, **368**, 32–38.
- Wingender, E., Bercz, G., Blöcker, H., Frank, R. and Mayer, H. (1989) *J. Biol. Chem.*, **264**, 4367–4373.

Received on April 21, 1994; revised on May 26, 1994

Note added in proof

While this article was in press, another report on the same gene, termed *odd Oz (odz)*, appeared in *Cell*, **77**, 587–598 (1994) by Levine et al. However, their interpretation of the data differs from ours in several points, leading to fundamental discrepancies. (i) We have no indications of a transmembrane spanning segment in the protein. (ii) The protein appears to be a large secreted proteoglycan and is not processed intracellularly or extracellularly to low molecular weight forms. (iii) According to our data, the phenotype is *odd-paired*-like, and not *odd-skipped* or *fushi-tarazu*-like. (iv) The gene is not a very-late acting pair-rule gene, rather it constitutes a secondary pair-rule gene.